

Implementing Spanlastics for Improving the Ocular Delivery of Clotrimazole: In vitro Characterization, Ex vivo Permeability, Microbiological Assessment and In vivo Safety Study

Manar Adel Abdelbari¹
 Shereen Sameh El-mancy¹
 Ahmed Hassen Elshafeey²
 Aly Ahmed Abdelbary^{2,3}

¹Department of Pharmaceutics and Industrial Pharmacy, Faculty of Pharmacy, October 6 University, Giza, Egypt;

²Department of Pharmaceutics and Industrial Pharmacy, Faculty of Pharmacy, Cairo University, Cairo, Egypt; ³School of Life and Medical Sciences, University of Hertfordshire Hosted by Global Academic Foundation, Cairo, Egypt

Purpose: The aim of this study was to encapsulate clotrimazole (CLT), an antifungal drug with poor water solubility characteristics, into spanlastics (SPs) to provide a controlled ocular delivery of the drug.

Methods: Span 60 was used in the formulation of SPs with Tween 80, Pluronic F127, or Kolliphor RH40 as an edge activator (EA). The presence of EA offers more elasticity to the membrane of the vesicles which is expected to increase the corneal permeation of CLT. SPs were prepared using ethanol injection method applying 3² complete factorial design to study the effect of formulation variables (ratio of Span 60: EA (w/w) and type of EA) on SPs characteristics (encapsulation efficiency percent (EE%), average vesicle size (VS), polydispersity index (PDI) and zeta potential (ZP)). Design-Expert software was used to determine the optimum formulation for further investigations.

Results: The optimum formulation determined was S1, which contains 20 mg of Tween 80 used as an EA and 80 mg of Span 60. S1 exhibited EE% = 66.54 ± 7.57%, VS = 206.20 ± 4.95 nm, PDI = 0.39 ± 0.00 and ZP = -29.60 ± 0.99 mV. S1 showed highly elastic sphere-shaped vesicles. Furthermore, S1 displayed a sustained release profile and a higher ex vivo permeation across rabbit cornea relative to CLT suspension. Also, S1 revealed superior inhibition of *Candida albicans* development compared to CLT suspension applying 2,3-bis (2-methoxy-4-nitro-5-sulphophenyl)-2H-tetrazolium-5-carboxanilide (XTT) reduction technique. Moreover, in vivo histopathological examination assured the safety of S1 after ophthalmic application in mature male albino rabbits.

Conclusion: Overall, the outcomes revealed the marked efficacy of SPs for ocular delivery of CLT.

Keywords: clotrimazole, spanlastics, edge activators, XTT reduction technique, ocular drug delivery

Introduction

Fungal infections of the eye have obviously increased lately and reported as a serious condition. This is considered a main cause of blindness, corneal scarring and illness if untreated.¹ The most repeatedly isolated organisms from the infected eye are *Candida*, *Fusarium* and *Aspergillus* species which mainly cause endogenous endophthalmitis, exogenous endophthalmitis, or fungal keratitis. Trauma is the most common predisposing factor followed by the administration of immunosuppressive agents and AIDS.²

Correspondence: Aly Ahmed Abdelbary
 Department of Pharmaceutics and Industrial Pharmacy, Faculty of Pharmacy, Cairo University, Kasr El-Aini, Cairo, 11562, Egypt
 Tel +20 1149005526
 Email aly.abdelbary@pharma.cu.edu.eg



Clotrimazole (CLT) is an azole agent with a topical potent antifungal action against infective yeasts and dermatophytes.³ It is a white crystalline powder with a molecular weight of 344.8 g/mol, insoluble in water (0.49 mg/L), sparingly soluble in ether and very soluble in polyethylene glycol 400, ethanol and chloroform. It is lipophilic with Log P of 6.1 and pKa of 6.7.⁴ CLT inhibits fungal cell growth by binding to the heme portion of dependent cytochrome P-450 lanosterol 14- α -demethylase enzyme, restrains 14- α -demethylase, inhibits ergosterol formation and causes the accumulation of poisonous methylated 14- α -sterols which together stop the cell growth. Topical forms of CLT are considered safe and without serious side effects.⁵ The clinical use of CLT is considered a challenge because of its poor water solubility. However, ocular drug delivery is also challenging because of the precorneal fast and extensive loss due to the high turnover of the tears leading to corneal penetration of very little amount of the drug reaching the intra-ophthalmic tissues. This recommends a high concentration and a frequent dosing of the antifungal treatment to reach the intended bioavailability.⁶ Encapsulation of CLT into surfactant-based nano-vesicular carriers can increase the drug corneal permeability, ocular residence time, improve bioavailability, decrease the dosing frequency and avoid undesirable side effects.³

Spanlastics (SPs) are highly elastic novel surfactant-based nanovesicles. They consist of an edge activator (EA) and a nonionic surfactant.⁷ They have the following advantages: chemical stability, target specificity, convenience and high patient compliance.⁶ SPs formulations are hypothesized to be a promising delivery system for the antifungal drug CLT over the conventional niosomes. The difference in structure between SPs and conventional niosomes is that niosomes consist of a non-ionic surfactant and cholesterol which is known to increase rigidity of the niosomal structure; which makes the vesicles less elastic.⁷ However, the presence of an EA in SPs formulations provides a great flexibility as the size and zeta potential of the formulations can be adjusted to suit the need using accessible and robust methodologies. The elasticity of the vesicles improves the corneal permeability of the drug as reported by ElMeshad and Mohsen⁸ regarding SPs as potential drug delivery system for both the anterior and posterior eye diseases.

The work in this study included the formulation and evaluation of CLT loaded SPs containing Span 60 with different three edge activators (Tween 80, Pluronic F127,

or Kolliphor RH40). Span 60 is a non-ionic stable lipophilic surfactant, with HLB value of 4.7. It is insoluble in water, soluble in ethanol (50 mg/mL), isopropanol, mineral oil and vegetable oil. However, Tween 80 is a hydrophilic non-ionic surfactant with HLB value of 15 and water solubility of 5–10 g/100 mL and it is liquid at 25°C. Pluronic F127 is a gel-based copolymer. It has a polar water-soluble group attached to a nonpolar water-insoluble hydrocarbon chain with HLB value of 22. Kolliphor RH40 is a paste at 25°C with HLB value of 14.⁹ A factorial design approach was used to study the effect of using different types and ratios of EAs on SPs properties: encapsulation efficiency percent (EE%), vesicle size (VS), polydispersity index (PDI) and zeta potential (ZP) followed by determination of the optimum formulation. Corneal permeability and elasticity of the optimum formulation were determined. Moreover, microbiological assessment for the optimum formulation was evaluated to measure the inhibition efficacy against *Candida albicans* compared with CLT suspension. The system safety was tested and compared to drug suspension.

Materials

CLT was provided kindly by Marcyrl Pharmaceutical Industries (Cairo, Egypt). Methanol (HPLC grade) and Span 60 were obtained from Merck-Schuchardt, Germany. Sodium dodecyl sulfate (SDS), potassium dihydrogen phosphate, dimethyl sulfoxide (DMSO), disodium hydrogen phosphate, sodium chloride and ethanol were purchased from El-Nasr Chemicals Company, Cairo, Egypt. Tween 80, Kolliphor RH40 and Pluronic F127 were obtained from Sigma Chemical Company, St. Louis, USA.

Methods

Preparation of CLT Loaded SPs

Ethanol injection technique reported by Kakkar and Kaur⁷ was used in the preparation of CLT SPs. CLT loaded SPs were prepared by changing Span 60: EA ratio (w/w) and type of EA. Ethanol was used as a solvent to dissolve CLT (20 mg) and Span 60 in a 60°C water bath. The solution was injected slowly into a five-fold larger aqueous phase containing the EA. The mixture was continuously stirred at 800 rpm at the same temperature until the full evaporation of ethanol forming SPs aqueous dispersion. Then, ultrasonic water-bath sonication was applied for five minutes to reach a proper VS in a sonicator water bath (Type USR3, Julabo Labortechnik,

Seelbach, West Germany) at 25°C. The SPs suspension was stored at 4°C till further investigation.^{10,11}

In vitro Characterization of CLT Loaded SPs

Measurement of EE% of CLT Loaded SPs

The percentage of CLT encapsulated into SPs was measured using indirect way by calculating the difference between the amount of CLT added in the vesicles and the amount remaining after separating the supernatant from the prepared SPs using cooling ultracentrifuge at 25,000 rpm for 1 hour at 4°C (Sigma 3–30 KS, Sigma Laborzentrifugen GmbH, Germany). The untrapped CLT concentration was determined by measuring the wavelength of the UV spectrum at 261 nm using ultraviolet (UV) spectrophotometer (Shimadzu, model UV-1601 PC, Kyoto, Japan). The EE% of the drug was calculated using this equation:^{10,12}

$$EE(\%) = \frac{\text{Total amount of CLT} - \text{Untrapped CLT}}{\text{Total amount of CLT}} \times 100$$

Mean VS, PDI and ZP Measurement

The average VS and PDI were measured using Zetasizer (Malvern Instrument Ltd., UK) applying the process of dynamic light-scattering. The electrophoretic mobility of the charged vesicles was observed to measure the ZP using the same instrument. All measurements were done at 25°C in triplicate after dilution of the formulations.¹³

Statistical Analysis

A complete 3² factorial design was employed using the software of Design-Expert (Version 7, Stat-Ease Inc., USA). Table 1 summarizes the design. Two factors each with 3 levels (X₁: Span 60: EA ratio (w/w)) and (X₂: EA Type) were investigated. The optimum formulation was chosen after the analysis of experimental results and calculation of desirability.

Characterization of the Optimum CLT Loaded SPs

Transmission Electron Microscope (TEM)

The morphology of the optimum CLT SPs vesicles was inspected using TEM (Joel JEM 1230, Tokyo, Japan) by employing a beam of high electron voltage to create a super magnified image. One drop of the dispersion was located on a carbon covered copper net, dried, then stained with 2% potassium phosphotungstate. After complete dryness, the sample was examined.^{14,15}

Table 1 The Independent Variables Levels Used to Formulate CLT Loaded SPs Utilizing (3²) Complete Factorial Design

Factors (Independent Variables)	Levels		
X ₁ : Span 60: EA ratio (w/w)	80: 20	70: 30	60: 40
X ₂ : Type of EA	Tween 80	Pluronic F127	Kolliphor RH40
Responses (Dependent Variables)	Desirability Constraints		
Y ₁ : EE%	Maximize		
Y ₂ : VS (nm)	Minimize		
Y ₃ : PDI	Minimize		
Y ₄ : ZP (mV)	Maximize (as absolute value)		

Abbreviations: CLT, clotrimazole; SPs, spanlastics; EA, edge activator; EE%, encapsulation efficiency percent; VS, vesicle size; PDI, polydispersity index; ZP, zeta potential.

Measurement of Elasticity

The elasticity of the optimum SPs formulation was determined by applying the extrusion technique explained by Van den Bergh et al.¹⁶ The formulation was diluted and extruded under a steady pressure of 2.5 bar (Haug Kompressoren AG; Büchi Labortechnik AG, Flawil, Switzerland) through a microporous filter of 220 nm pore size (Jinteng Experiment Equipment Co., Ltd, China).¹⁷ Zetasizer Nano ZS was used to measure VS pre- and post-extrusion and then the percentage alteration in VS was calculated.

The Storage Effect on the Optimum SPs

The optimum SPs formulation was stored for 90 days at 25°C and 4°C. Samples were taken from fresh SPs, after 45 days and after 90 days. The storage effect was evaluated by the comparison between the first and the after storage results in respect of EE%, VS, PDI and ZP.¹⁸ Student's *t*-test was used to analyze the results statistically using SPSS[®] program 22.0 (USA). A significant difference was considered at $P \leq 0.05$.

In vitro Release Profile

The release of CLT from the optimum SPs formulation was done using a cellulose-based membrane of 12,000–14,000 Dalton mass cut off (Spectra/Pro, Spectrum Laboratories, Inc., USA). A dialysis tube was created by fixing the membrane on a top-cut plastic tube at one end using rubber band. Then, 2 mL of the preparation (equivalent to 4 mg CLT) was located in the dialysis tube that was

attached to the dissolution apparatus II shaft (Distek, 2500, USA) and adjusted carefully. A volume of 20 mL phosphate buffer saline (pH 7.4) with 1% SDS was used as the release medium. The temperature was kept at $37 \pm 0.5^\circ\text{C}$ and the stirring speed was regulated to 100 rpm. The receptor part was enclosed to limit the release medium evaporation. One mL aliquot was withdrawn at time 0.5, 1, 2, 4, 6, 8, 10 and 12 hours. Then, 1 mL of the fresh medium was added as a replacement to keep the volume constant. A 0.22 μm sterile syringe filter was used for the filtration of the samples and CLT content was analyzed using HPLC.¹⁹ The cumulative amount of CLT released at each time interval was calculated and the release profile of the optimum formulation was obtained by plotting the percentage of CLT released at each time point vs time to construct the drug release profile graph.

Release Kinetic Mechanisms

Release behavior of CLT from the optimum formulation was kinetically evaluated using various kinetic equations. The results were fitted into different mathematical equations like zero-order kinetics, first-order kinetics, second-order kinetics, third-order kinetics and diffusion models and were used for the analysis of the release data. The correlation coefficient (R^2) was determined for each model²⁰.

Ex vivo Studies

Preparation of the Cornea

All the study protocols on animals were accepted by the Research Ethics Committee, Faculty of Pharmacy, Cairo University, Egypt (approval number PT 212). An average weight mature male albino rabbits were anesthetized and killed. The eyes were explicated and the corneas were cut off immediately and washed using fresh saline. The corneal permeation experiment was done within half an hour of killing the rabbits.^{7,21}

Corneal Permeation Study

A side by side diffusion cell device was used to study permeation of CLT through fresh rabbit cornea. The temperature was maintained at 37°C . The cornea was located cautiously among the donor pool and receptor pool keeping the corneal epidermis towards the donor one. A 20 mL of fresh phosphate buffer saline (PH 7.4) with 1% SDS was prepared as receptor medium and 0.5 mL of the preparation was added in the donor pool. The stirring was kept continuous and 1 mL of the receptor medium

was withdrawn after fixed time. A replacement of the fresh medium was added after each aliquot to keep the volume constant.²² The measurement of the withdrawn samples was done using HPLC. The following equation was used to quantify the cumulative CLT permeated percent at different time points:²³

$$Q_n = \frac{C_n \times V_r + \sum_{i=1}^{n-1} C_i \times V_s}{\text{initial drug content}} \times 100$$

Where:

Q_n : Cumulative drug permeated percent.

C_n : Drug concentration in the receiver.

V_r : Receiver medium volume.

V_s : Sample volume.

$\sum_{i=1}^{n-1} C_i$: Total previously measured concentrations.

Determination of CLT Using HPLC

A validated HPLC method was used in the measurement of CLT.²⁴ The HPLC system (LC-20AD, Shimadzu, Japan) consisted of reverse-phase column C_{18} (4.6 cm x 250 mm) (SC-150, Germany) and UV-sensor running at 210 nm. The elution mobile phase used was (80:20 v/v) methanol: water with 0.8 mL/minute flow rate. The time of CLT retention was 9.5 minutes. The approach was confirmed and validated for good linearity, selectivity, accuracy and precision.

Microbiological Assay of CLT SPs Applying the Reduction Technique of 2,3-Bis-(2-Methoxy-4-Nitro- 5-Sulfophenyl)-2H-Tetrazolium -5-Carboxanilide (XTT)

The minimum concentration that restrains the development of *Candida albicans* (ATCC 90028) completely is called the minimum inhibitory concentration (MIC) value. A micro-well dilution assay was used to determine MIC using prepared inoculums with concentrations of 10^6 CFU/ mL. DMSO was used for the dilution of CLT suspension, plain SPs containing no drug and optimum SPs formulation in a 96 well plate.²⁵ The microplate wells were filled with 40 μL of brain heart infusion as the growth medium, 50 μL of formulations after dilution and 10 μL of the inoculum. DMSO was considered as a negative control.

The incubation of the plates continued at 37°C for 24 hours followed by the addition of 40 μL of tetrazolium salt followed by an hour of incubation at same temperature in the dark. Any reduction of XTT appeared as a change in color and measured at 492 nm using the microplate

photometer (Tecan Sunrise absorbance reader, UK). The percent of inhibition was measured using the following equation:²⁶

The percentage of

$$\text{inhibition} = 1 - \left(\frac{\text{average of test wells}}{\text{average of control wells}} \right) \times 100$$

In vivo Histopathological Investigation

The safety of the optimum SPs formulation was evaluated using three mature male albino rabbits with an average weight of 3.0 ± 0.5 Kg. The use and handling of rabbits complied with the EU directive 2010/63/EU for animal experiment. The rabbits were kept in cages at a temperature of 22°C and relative humidity of 55%. The rabbits had free access to water, supplied with standard diet and were put in a dark: light cycle of 12 hrs each. Rabbits were left for 7 days for adaptation before experiments. The formulations were sterilized using gamma-irradiation. Samples were sterilized in type I glass vials using a ^{60}Co irradiator offered at National Center for Radiation Research & Technology, secondary to Atomic Energy Authority, Nasr City, Egypt.⁸ The rabbits were divided into 3 groups; group 1 was considered as Control group, CLT suspension was applied to group 2 and group 3 was given the optimum SPs formulation. For a week, three doses were dripped daily in the left eye of every rabbit. The right ones were considered as a control. Eventually, on the seventh day, the rabbits were anesthetized and killed. A separation of the eyeballs was done and were then washed with normal saline and fixed with 10% formal saline for a day. The tissue samples were cleaned using double-distilled water then desiccated using alcohol. Then, the specimens were placed in melted paraffin wax, solidified in blocks and kept at 56°C for 24 hours.¹⁰ Histopathological

abnormalities were examined microscopically after cutting sections (3–4 mm) by a sliding microtome (Leica Microsystems SM2400, Cambridge, UK), deparaffinizing and staining using hematoxylin and eosin.

Results and Discussion

Investigation of Factorial Design

A complete factorial design was applied and analyzed statistically to identify the effect of some variables on the features of the formulated SPs since it is considered a suitable method for analysis.²⁷ Factors and levels in this manuscript were selected carefully after several trials to accomplish the possible independent variables arranges. The independent variables and the measured responses of all SPs formulations are illustrated in Table 2 that demonstrates 9 experimental formulations (S1–S9) that combine 2 factors with 3 levels. Adequate precision is the ratio between signal and noise. As desired, a ratio > 4 was gained in all responses²⁸ as shown in Table 3. The quality of the model is also affected by the predicted R^2 .^{29,30} The adjusted and predicted (R^2) must be in rational agreement³¹ and that is revealed in all the studied responses (Table 3).

Formulation Variables Effect on the EE% of CLT Loaded SPs

As shown in Table 2, CLT was successfully entrapped in all the prepared formulations. The effect of Span 60: EA ratio (w/w) and type of EA on EE% are demonstrated as linear plot in Figure 1. The analysis of the data statistically revealed significant difference ($P < 0.05$) between EE% of SPs prepared using the three Span 60: EA ratios (w/w) (80:20), (70:30) and (60:40). When increasing the amount of EA, the EE% increases. This is caused by the effect of EA in forming a layer that increases the vesicles interface stability and giving

Table 2 Measured Responses of CLT Formulations of the Experimental Complete 3^2 Factorial Design

Formulations	X ₁ Span 60: EA Ratio	X ₂ Type of EA	Y ₁ EE%	Y ₂ VS (nm)	Y ₃ PDI	Y ₄ ZP (mV)
S1	80: 20	Tween 80	66.54 ± 7.57	206.20 ± 4.95	0.39 ± 0.00	-29.60 ± 0.99
S2	80: 20	Pluronic F127	67.38 ± 0.00	366.70 ± 102.00	0.56 ± 0.10	-22.10 ± 0.49
S3	80: 20	Kolliphor RH40	40.96 ± 24.25	356.10 ± 8.84	0.59 ± 0.09	-29.40 ± 0.49
S4	70: 30	Tween 80	21.91 ± 8.76	162.10 ± 0.14	0.36 ± 0.03	-29.00 ± 6.51
S5	70: 30	Pluronic F127	33.34 ± 4.38	227.10 ± 2.69	0.36 ± 0.05	-28.20 ± 1.41
S6	70: 30	Kolliphor RH40	97.74 ± 1.51	411.30 ± 13.00	0.81 ± 0.05	-26.10 ± 2.83
S7	60: 40	Tween 80	94.52 ± 0.00	309.50 ± 5.23	0.44 ± 0.01	-25.40 ± 0.21
S8	60: 40	Pluronic F127	64.53 ± 4.38	179.00 ± 3.96	0.33 ± 0.04	-27.20 ± 0.64
S9	60: 40	Kolliphor RH40	80.12 ± 5.90	245.40 ± 1.13	0.47 ± 0.00	-21.20 ± 0.57

Notes: All the prepared SPs contained 10 mL CLT nanosuspension (equivalent to 20 mg drug). Data are presented as mean \pm SD (n=3).

Abbreviations: CLT, clotrimazole; EA, edge activator; EE%, encapsulation efficiency percent; VS, vesicle size; PDI, polydispersity index; ZP, zeta potential; SPs, spanlastics.

Table 3 The Statistics Summary of Complete Factorial Design (3²) Used for Optimization of SPs Formulations

Responses	R ²	Adjusted R ²	Predicted R ²	Adequate Precision	Significant Factors
Y ₁ : EE%	0.93	0.87	0.73	11.39	X ₁ , X ₂
Y ₂ : VS (nm)	0.92	0.85	0.69	10.12	X ₁ , X ₂
Y ₃ : PDI	0.94	0.89	0.76	13.23	X ₁ , X ₂
Y ₄ : ZP (mV)	0.74	0.50	-0.05	4.82	—

Abbreviations: SPs, Spanlastics; EE%, encapsulation efficiency percent; VS, vesicle size; PDI, polydispersity index; ZP, zeta potential.

more room inside SPs to hold more drug.³² Three EAs were used in the preparation of CLT SPs namely Tween 80, Pluronic F127 and Kolliphor RH40. Kolliphor RH40 showed the highest mean drug entrapped (72.94%) followed by Tween 80 (60.99%) and Pluronic F127 (55.08%). The explanation of these results is based on the EAs hydrophile-lipophile balance (HLB) values which are 14, 15 and 22 for Kolliphor RH40, Tween 80 and Pluronic F127, respectively. Values of HLB are related to the EA alkyl chain length.⁸ The longer the alkyl chain is, the less HLB value which indicates that EA is more hydrophobic,^{33,34} hence forming less hydrophilic holes and decreasing the fluidity of the membrane by decreasing the bilayers amphiphilic property. This results in increased EE%.¹⁷

Formulation Variables Effect on VS of CLT Loaded SPs

The VS of the formulated SPs ranged from 162.10 to 411.30 nm. All preparations had a VS < 5 μm which is perfect for ophthalmic administration.³⁵ Analysis of the data statistically showed a significant impact ($P < 0.05$)

of Span 60: EA ratio (w/w) on mean VS. Results are demonstrated as linear plot at Figure 1. Table 2 showed that Span 60: EA ratio (w/w) (60:40) gave the smallest VS, giving a mean of 244.63 nm. This is probably caused by the reduction in the interfacial tension due to the EA higher concentration facilitating particle partition and formation of smaller vesicles.³⁶

Statistical analysis also showed a significant effect ($P < 0.05$) of EA type on mean VS. The smallest VS was detected in the vesicles prepared using Tween 80 as an EA. This is might be due to steric repulsion rendered by its molecules which minimizes the aggregation of the vesicles.⁹ Tween 80 might also act as stabilizing agent during vesicles formation that results in reduced surface energy causing inhibition of crystal growth and reduction in VS.³⁷ On the other hand, SPs formulated using Kolliphor RH40 as an EA had the largest VS. This behavior might be attributed to the branched structure and relative bulkiness of Kolliphor RH40 molecules leading to increased size of the vesicles. The physical state may

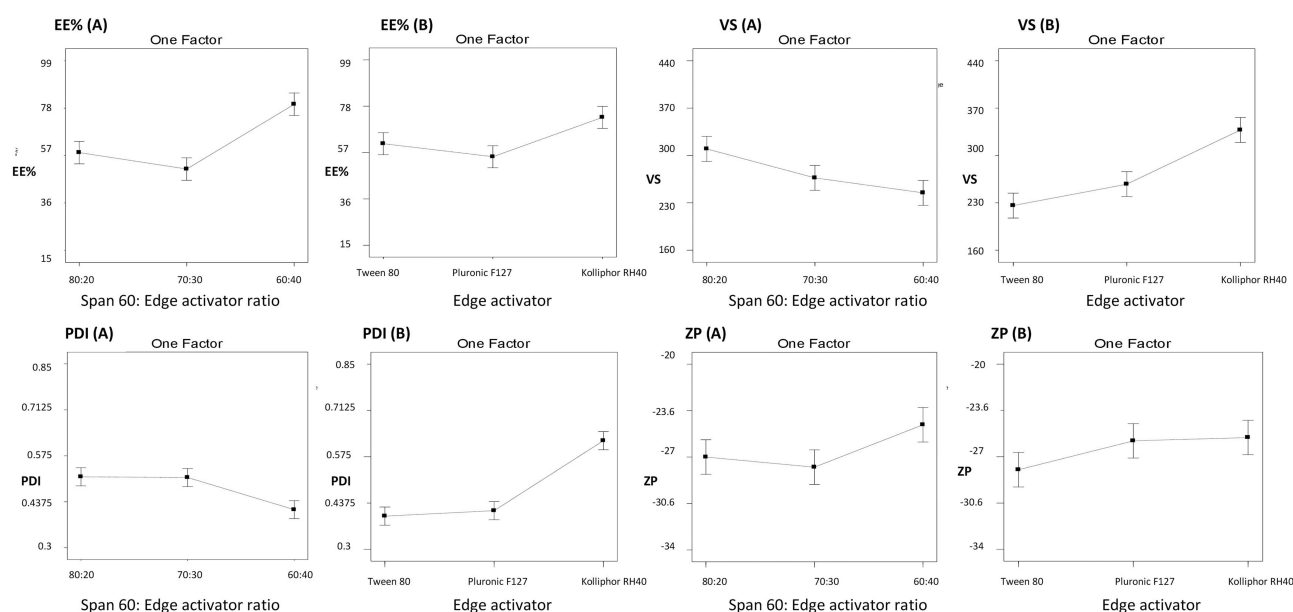


Figure 1 Linear correlation plots presenting the effect of (A) Span 60: EA ratio and (B) EA type on the following parameters: EE%, VS, PDI and ZP.

Abbreviations: EA, edge activator; EE%, encapsulation efficiency percent; VS, vesicle size; PDI, polydispersity index; ZP, zeta potential.

also explain the size difference where Tween 80 has a liquid nature while Kolliphor RH40 is a paste at 25°C.⁹

Formulation Variables Effect on PDI

PDI is the size distribution width of the formulation. Its value varies from 0 to 1. A homogeneous VS distribution shows low PDI value while a larger PDI indicates lower VS uniformity.³⁶ Results are demonstrated as linear plot in Figure 1. As shown in Table 2, PDI measurements were between 0.33 and 0.81, showing that the vesicular preparations had a variable homogeneity to a certain degree. Factorial analysis showed that the ratio (w/w) of Span 60: EA significantly affects PDI ($P < 0.05$). The vesicles prepared using the ratio (60:40) had the lowest PDI. This is probably due to the increased EA amount that reached maximum coverage to the vesicles surface. Also, this could be attributed to the effect of steric resistance of the EA by forming an adsorption layer on the particle surface.³⁸

Likewise, factorial analysis revealed that EA type significantly affected PDI ($P < 0.0001$). The PDI results showed that the factors which affected the VS of the SPs also affected the PDI of the dispersions. The PDI was lowest in SPs containing Tween 80 which had the smallest VS. Also, Kolliphor RH40 containing SPs had the highest PDI. This can be explained by the increased size of the vesicles caused by the relative bulkiness of Kolliphor RH40 and the repulsion between the bilayers molecules therefore increasing PDI.⁹

Formulation Variables Effect on ZP

ZP is indication of colloidal dispersions stability, it is the measurement of all charges gained by vesicles. When ZP value exists between ± 30 mV the system is stable due to the presence of sufficient electric repulsive force between particles.¹⁰ The Span type has an important role in predicting the vesicular formulation stability. The most suitable surfactant is Span 60 and this is due to the saturation of the alkyl chains present in it which gives the vesicles higher stability.³⁹ In this manuscript, values of ZP obtained ranged from -21.20 to -29.60 mV (Table 2). Formulations exhibited a negative zeta potential that caused a repulsion between the vesicle bilayers. This could be attributed to increasing OH^- ion concentration present in Span 60 and EAs used producing highly negative charges.⁴⁰ Factorial analysis revealed a non-significant effect of Span 60: EA ratio (w/w) and EA type on ZP. Results are presented as linear plot in Figure 1.

Determination of the Optimum SPs Formulation

Complete factorial design was applied using the results of the 9 prepared SPs formulations to determine the optimum one using Design-Expert software. The optimum formulation criteria was to achieve highest EE% and ZP (absolute value) and lowest VS and PDI values. This was achieved in formulation S1 with a desirability of 0.74. S1 was formulated using Span 60: EA ratio (w/w) (80:20) using Tween 80 as an EA and showed EE% of $66.54 \pm 7.57\%$, VS of 206.20 ± 4.95 nm, PDI of 0.39 ± 0.00 and ZP of -29.60 ± 0.99 mV.

Characterization of the Optimum CLT Loaded SPs

Transmission Electron Microscopy (TEM)

TEM is used to determine the shape, size and lamellarity of vesicles.⁴¹ TEM examination of CLT optimum formulation (S1) showed spherical drug nanoparticles with no signs of aggregation as shown in Figure 2. Also, the particle diameter of the vesicles observed by TEM micrographs agreed with that obtained by the Zetasizer.

Elasticity Measurement

The degree of elasticity of SPs vesicular formulation is very important parameter as it shows the ability of elastic vesicles to cross the mucus membrane by compressing themselves.⁸ S1 elasticity was examined for any deformable characteristics. The VS were 206.20 ± 4.95 and 176.20 ± 1.27 nm before and after extrusion, respectively. The results revealed a very small change (14.6%) in average VS, indicating a high elastic vesicles. This is probably due to the high flexibility and non-bulky alkyl chain of Tween 80 that leads to the formation of an elastic vesicle membrane.¹⁷

Stability Study of the Optimum SPs

Results showed good stability of S1 after storage. The appearance of stored CLT vesicles did not record any significant variations. No significant changes concerning EE%, VS, PDI and ZP of stored SPs vesicles appeared in the stability analysis ($P > 0.05$) in relation to the fresh ones as presented in Table 4.

In vitro Release Profile

In vitro release profile of the drug is a good prediction of the way a delivery system works in ideal conditions and expects its in vivo performance.⁴² The experiment was done using

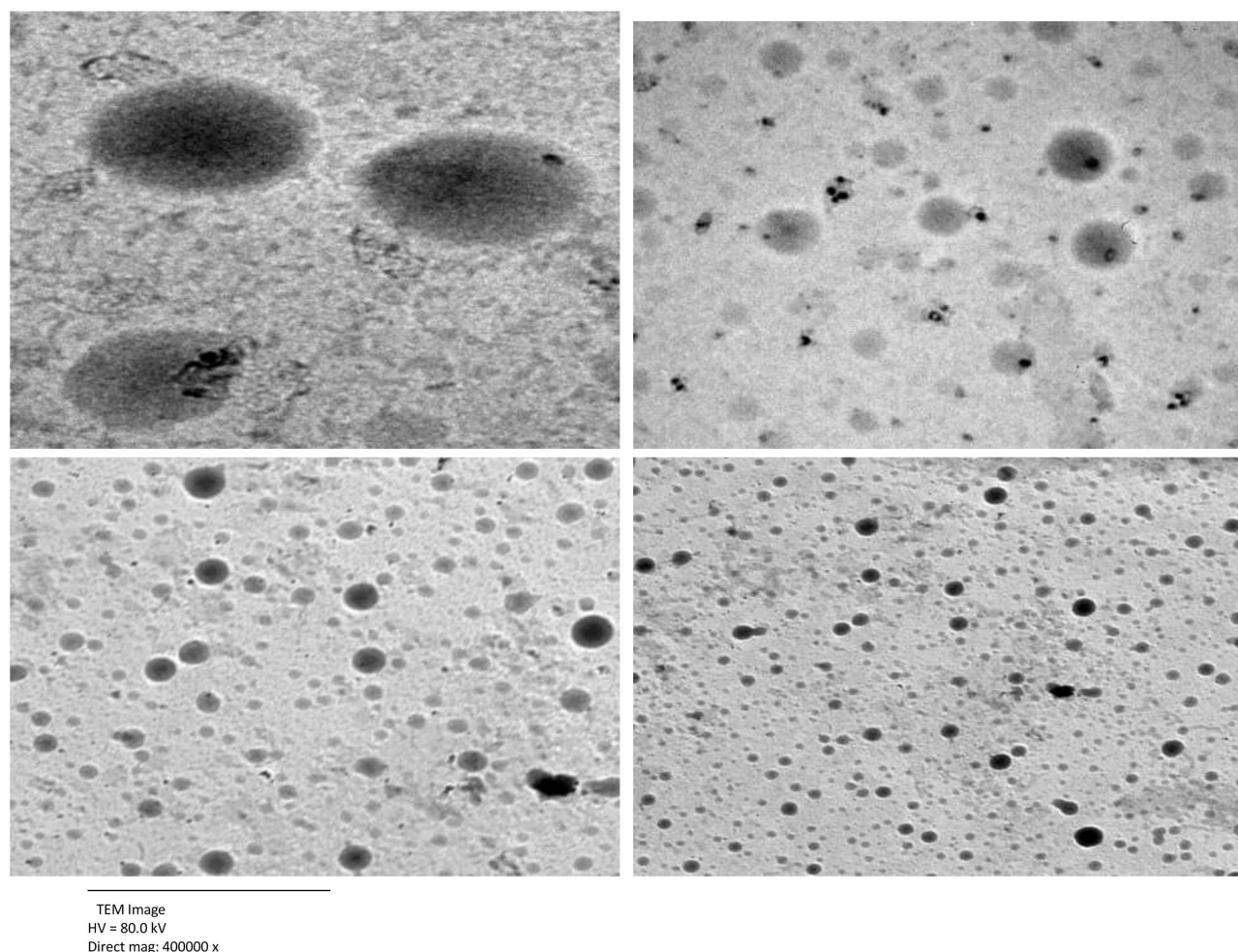


Figure 2 The optimum SPs formulation (S1) transmission electron micrograph.
Abbreviation: SPs, Spanlastics.

S1 compared to CLT suspension. The percentage of drug released from the formulations was calculated for further comparison. Figure 3 presents the release profile of CLT from S1 and drug suspension. The results showed that SPs had a slower release than drug suspension. The percentage of CLT released in 6 hours from S1 were significantly lower in relation to CLT suspension ($P < 0.05$) applying

independent Student's *t*-test using SPSS[®] program 22.0. These results could be attributed to the presence of the alkyl chain in Tween 80 which causes a lower release rate as it increases the bilayer hydrophobicity.⁴³ This also may be due to the Span 60 high transition temperature (TC) that forms a more rigid less permeable bilayer. Also, Span 60 has long-chain length leading to more stable vesicles which gave

Table 4 Effect of Storage on Physical Properties of the Optimum Formulation S1

Parameter	S1 Fresh	S1 After 45 Days at 4°C	S1 After 45 Days at 25°C	S1 After 90 Days at 4°C	S1 After 90 Days at 25°C
EE%	66.54 ± 7.57	66.68 ± 1.90	68.82 ± 1.18	66.67 ± 2.20	67.60 ± 3.68
VS (nm)	206.20 ± 4.95	210.30 ± 7.42	207.40 ± 3.96	219.00 ± 2.19	211.50 ± 0.78
PDI	0.39 ± 0.00	0.47 ± 0.03	0.46 ± 0.02	0.42 ± 0.02	0.40 ± 0.03
ZP (mV)	-29.60 ± 0.99	-30.60 ± 0.07	-28.90 ± 1.34	-31.00 ± 0.14	-30.00 ± 1.13

Note: Data are presented as mean ± SD ($n = 3$).

Abbreviations: EE%, encapsulation efficiency percent; VS, vesicle size; PDI, polydispersity index; ZP, zeta potential.

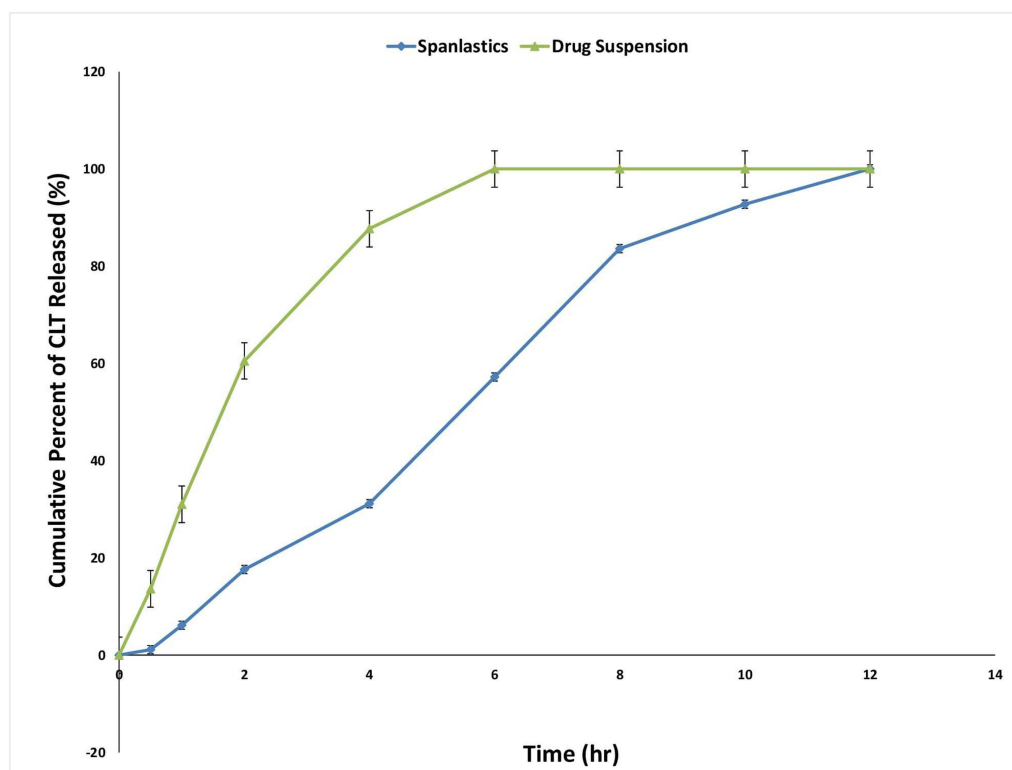


Figure 3 In vitro release study of CLT formulations.

Abbreviation: CLT, clotrimazole.

delayed drug release.⁴⁴ The comparative data indicates that vesicular encapsulation of CLT controls and sustains its release for a longer time interval as reported by Ruckmani et al.⁴⁵ This in turn increases bioavailability, decreases the drug dosage regimen and causes a reduction in the toxicity of the drug.

Kinetic Analysis of Drug Release

Table 5 presents the release kinetic modeling and correlation coefficients (R^2) calculated for the investigated formulation (S1). Kinetic analysis of the release data showed that R^2 value was the highest in the zero-order model. Therefore, S1 followed zero-order release kinetics representing concentration independent drug release. This may be explained by the high concentration of Tween 80 that formed strong

diffusional gel matrix allowing the release of the drug in a controlled way independent of concentration.⁴⁶

Corneal Permeability Study

Corneal permeation studies reflect the action of an ophthalmic drug delivery system inside the body.²¹ Corneas of mature albino male rabbits were used to measure the permeation of CLT from S1. Figure 4 presents the cumulative percentage of CLT permeated as a function of time from S1 in relation to CLT suspension. The percentage of CLT permeated in 8 hours from S1 was significantly higher than CLT permeated from drug suspension at the same time ($P < 0.05$) utilizing Student's *t*-test using SPSS[®] program 22.0. The resulted permeability percentages are in good correlation with the elasticity results which provided the vesicles

Table 5 Kinetics of CLT Release from S1 According to Different Kinetic Models

Formulation	Zero Order	First Order	Second Order	Third Order	Diffusion
	Correlation Coefficient (R^2) *				
S1	0.98 ± 0.00	0.77 ± 0.03	0.44 ± 0.03	0.34 ± 0.04	0.97 ± 0.03

Note: *Mean ± SD (n=3).

Abbreviation: CLT, clotrimazole.

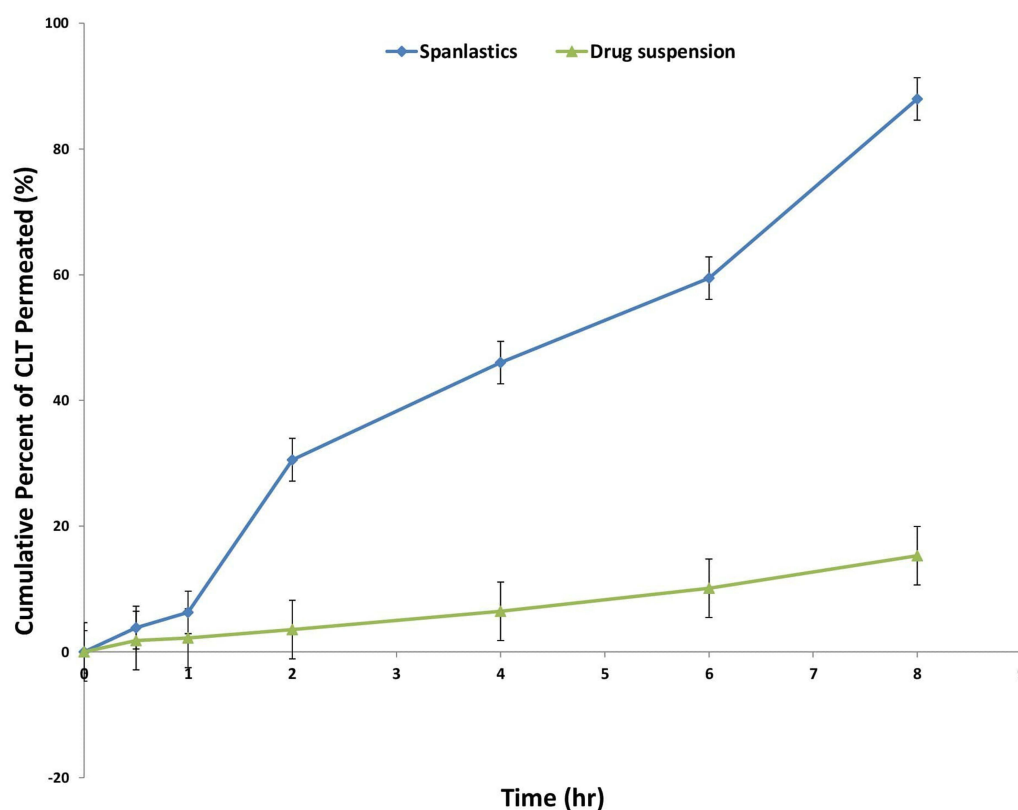


Figure 4 Ex vivo corneal permeability of CLT formulations.

Abbreviation: CLT, clotrimazole.

with greater membrane flexibility allowing them to efficiently penetrate the cornea.⁴⁷ The presence of Tween 80 as EA caused the high capability of SPs vesicles to compress themselves through the cornea because of its tendency for highly curved structures giving SPs high permeability.⁹ Furthermore, SPs after compressing through the cornea will pass in an intact form through aqueous humor achieving the antifungal activity of CLT.

Microbiological Assay of CLT SPs for Treating *Candida albicans*

MIC Determination via XTT Reduction Technique

The in vitro antifungal test was done to detect *Candida albicans* being the most common cause of human fungal infections.⁴⁸ Candida activity can be measured quantitatively using XTT reduction technique unlike the agar diffusion technique. The reduction process of XTT releases intracellular formazan compound that can be measured calorimetrically reflecting the cell activity.^{47,49} Figure 5 presents the antifungal activity of CLT suspension, non-medicated S1 and CLT loaded S1. S1 had the lowest MIC of 0.98 µg/mL while CLT suspension and non-medicated S1

MICs were 7.81 and 1000 µg/mL, respectively. The effectiveness of the formulation increases when MIC decreases which shows better antifungal activity. S1 accomplished around eight-times less MIC than CLT suspension. This might be due to the ultimate diffusion of CLT and its high discharge from S1 compared with CLT suspension.¹⁷

In vivo Studies

Histopathological Ocular Examination

Histopathological examination using light microscopy was done for the stained sections of ocular tissues of male albino rabbits. All three groups; group 1: Control group, group 2: treated with CLT suspension and group 3: treated with S1 showed no histopathological change in the iris, sclera, retina, or cornea (Figure 6). This ensures the safety of CLT SPs for ocular delivery.

Conclusions

In this study, we prepared SPs as a novel nanovesicles for the usage of CLT to treat ocular fungal infections. The preparation of CLT loaded SPs was done using ethanol injection method. A complete 3² factorial design was utilized to set

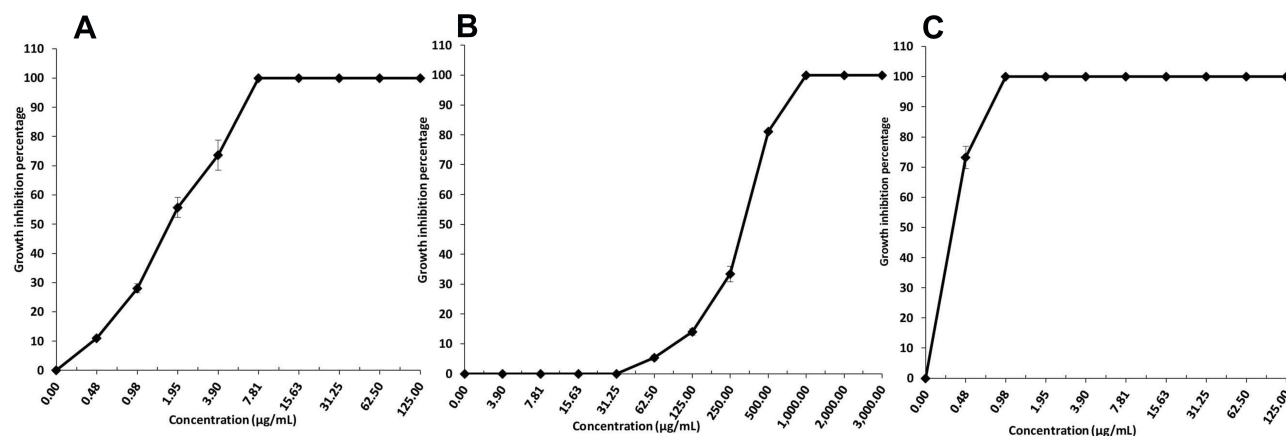


Figure 5 Microbiological assay of (A) CLT suspension, (B) Non-medicated S1 and (C) S1 for the treatment of *Candida albicans* infection. Data are presented as mean \pm SD, (n=3).

Abbreviation: CLT, clotrimazole.

experimental design and to determine the optimum formulation (S1) that had spherical morphology, high EE% and small VS. S1 also had a sustained in vitro release profile in relation to CLT suspension. Moreover, the corneal permeability study of the investigated SPs showed that S1 had a higher drug permeation than CLT suspension. These outcomes along with SPs high elasticity are essential requirements for the

absorption by the cornea. Microbiological evaluation of S1 showed a high activity against *Candida albicans* relative to CLT suspension. Additionally, the administration of S1 to the corneas of the study rabbits confirmed the non-irritant nature of SPs vesicles. Briefly, SPs vesicles offer convenient and promising system for the delivery of CLT to cure ophthalmic fungal infections.

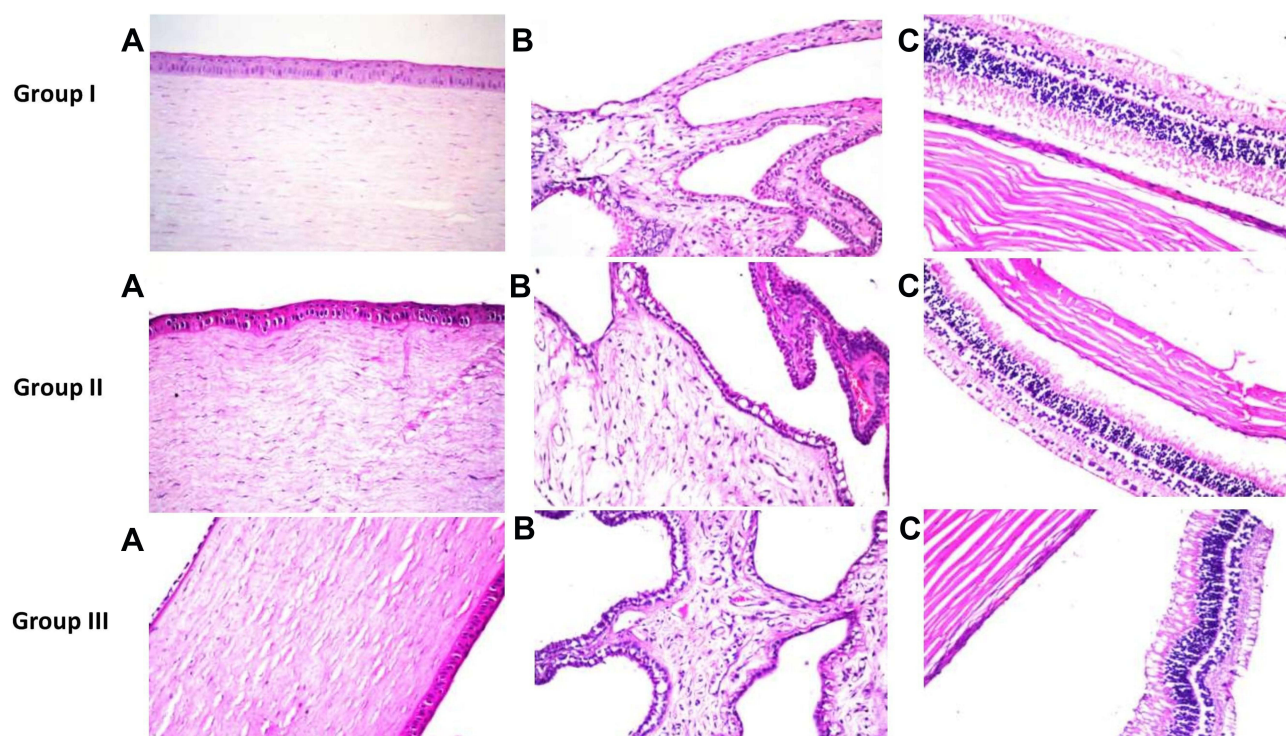


Figure 6 Photomicrographs presenting histopathological sections (stained by hematoxylin and eosin) of normal untreated rabbit eye (group I), rabbit eye treated with CLT suspension (group 2) and rabbit eye treated with S1 (group 3). (A) Shows histological structure of the cornea, (B) Shows histological structure of the iris and (C) Shows histological structure of the sclera, retina and choroid.

Abbreviation: CLT, clotrimazole.

Disclosure

The authors report no conflicts of interest for this work.

References

1. Zubairu Y, Negi LM, Iqbal Z, Talegaonkar S. Design and development of novel bioadhesive niosomal formulation for the transcorneal delivery of anti-infective agent: in-vitro and ex-vivo investigations. *Asian J Pharm Sci*. 2015;10(4):322–330. doi:10.1016/j.ajps.2015.02.001
2. Thomas PA. Fungal infections of the cornea. *Eye*. 2003;17(8):852–862. doi:10.1038/sj.eye.6700557
3. Basha M, Abd El-Alim SH, Shamma RN, Awad GEA. Design and optimization of surfactant-based nanovesicles for ocular delivery of clotrimazole. *J Liposome Res*. 2013;23(3):203–210. doi:10.3109/08982104.2013.788025
4. Bolla PK, Meraz CA, Rodriguez VA, et al. Clotrimazole loaded ufosomes for topical delivery: formulation development and in-vitro studies. *Molecules*. 2019;24(17):3139. doi:10.3390/molecules24173139
5. Crowley PD, Gallagher HC. Clotrimazole as a pharmaceutical: past, present and future. *J Appl Microbiol*. 2014;117(3):611–617. doi:10.1111/jam.12554
6. Liu Y, Wang Y, Yang J, Zhang H, Gan L. Cationized hyaluronic acid coated spanlastics for cyclosporine A ocular delivery: prolonged ocular retention, enhanced corneal permeation and improved tear production. *Int J Pharm*. 2019;565(100):133–142. doi:10.1016/j.ijpharm.2019.05.018
7. Kakkar S, Kaur IP. Spanlastics-a novel nanovesicular carrier system for ocular delivery. *Int J Pharm*. 2011;413(1–2):202–210. doi:10.1016/j.ijpharm.2011.04.027
8. ElMeshad AN, Mohsen AM. Enhanced corneal permeation and antimycotic activity of itraconazole against *Candida albicans* via a novel nanosystem vesicle. *Drug Deliv*. 2016;23(7):2115–2123. doi:10.3109/10717544.2014.942811
9. Shaker S, Gardouh A, Ghorab M. Factors affecting liposomes particle size prepared by ethanol injection method. *Res Pharm Sci*. 2017;12(5):346–352. doi:10.4103/1735-5362.213979
10. Abdelbary AA, Abd-Elsalam WH, Al-mahallawi AM. Fabrication of novel ultra-deformable bilosomes for enhanced ocular delivery of terconazole: in vitro characterization, ex vivo permeation and in vivo safety assessment. *Int J Pharm*. 2016;513(1–2):688–696. doi:10.1016/j.ijpharm.2016.10.006
11. Mosallam S, Sheta NM, Elshafeey AH, Abdelbary AA. Fabrication of highly deformable bilosomes for enhancing the topical delivery of terconazole: in vitro characterization, microbiological evaluation, and In Vivo Skin Deposition Study. *AAPS PharmSciTech*. 2021;22(2):74. doi:10.1208/s12249-021-01924-z
12. Al-mahallawi AM, Fares AR, Abd-Elsalam WH. Enhanced permeation of methotrexate via loading into ultra-permeable niosomal vesicles: fabrication, statistical optimization, ex vivo studies, and in vivo skin deposition and tolerability. *AAPS PharmSciTech*. 2019;20(5):171. doi:10.1208/s12249-019-1380-5
13. Elsherif NI, Al-Mahallawi AM, Abdelkhalek AA, Shamma RN. Investigation of the potential of nebulivolol hydrochloride-loaded chitosomal systems for tissue regeneration: in vitro characterization and in vivo assessment. *Pharmaceutics*. 2021;13(5):700. doi:10.3390/pharmaceutics13050700
14. Emad Eldeeb A, Salah S, Ghorab M. Proniosomal gel-derived niosomes: an approach to sustain and improve the ocular delivery of brimonidine tartrate; formulation, in-vitro characterization, and in-vivo pharmacodynamic study. *Drug Deliv*. 2019;26(1):509–521. doi:10.1080/10717544.2019.1609622
15. Ahmed MA, Al-mahallawi AM, El-Helaly SN, Abd-Elsalam WH. The effect of the saturation degree of phospholipid on the formation of a novel self-assembled nano-micellar complex carrier with enhanced intestinal permeability. *Int J Pharm*. 2019;569:118567. doi:10.1016/j.ijpharm.2019.118567
16. van den Bergh BAI, Wertz PW, Junginger HE, Bouwstra JA. Elasticity of vesicles assessed by electron spin resonance, electron microscopy and extrusion measurements. *Int J Pharm*. 2001;217(1–2):13–24. doi:10.1016/S0378-5173(01)00576-2
17. El Zaafarany GM, Awad GAS, Holayel SM, Mortada ND. Role of edge activators and surface charge in developing ultra-deformable vesicles with enhanced skin delivery. *Int J Pharm*. 2010;397(1–2):164–172. doi:10.1016/j.ijpharm.2010.06.034
18. Zeb A, Qureshi OS, Kim HS, Cha JH, Kim HS, Kim JK. Improved skin permeation of methotrexate via nanosized ultra-deformable liposomes. *Int J Nanomedicine*. 2016;11:3813–3824. doi:10.2147/IJN.S109565
19. Omar S, Ismail A, Hassanin K, Hamdy S. Formulation and evaluation of cubosomes as skin retentive system for topical delivery of clotrimazole. *J Adv Pharm Res*. 2019;3(2):68–82. doi:10.21608/aprh.2019.9839.1079
20. Fetihi G, Allam A. Sublingual fast dissolving niosomal films for enhanced bioavailability and prolonged effect of metoprolol tartrate. *DDDT*. 2016;10:2421–2433. doi:10.2147/DDDT.S113775
21. Qi J, Dai Z, Lu Y, Wu W. Liposomes containing bile salts as novel ocular delivery systems for tacrolimus (FK506): in vitro characterization and improved corneal permeation. *Int J Nanomedicine*. 2013;8:1921. doi:10.2147/IJN.S44487
22. Battaglia L, D'Addino I, Peira E, Trotta M, Gallarate M. Solid lipid nanoparticles prepared by coacervation method as vehicles for ocular cyclosporine. *J Drug Deliv Sci Technol*. 2012;22(2):125–130. doi:10.1016/S1773-2247(12)50016-X
23. Said M, Aboelwafa AA, Elshafeey AH, Elsayed I. Central composite optimization of ocular mucoadhesive cubosomes for enhanced bioavailability and controlled delivery of voriconazole. *J Drug Deliv Sci Technol*. 2021;61:102075. doi:10.1016/j.jddst.2020.102075
24. Esposito E, Sguizzato M, Bories C, Nastruzzi C, Cortesi R. Production and characterization of a clotrimazole liposphere gel for candidiasis treatment. *Polymers*. 2018;10(2):1–16. doi:10.3390/polym10020160
25. Tunney MM, Ramage G, Field TR, Moriarty TF, Storey DG. Rapid colorimetric assay for antimicrobial susceptibility testing of *Pseudomonas aeruginosa*. *Antimicrob Agents Chemother*. 2004;48(5):1879–1881. doi:10.1128/aac.48.5.1879-1881.2004
26. Mosallam S, Ragaie MH, Mofteh NH, Elshafeey AH, Abdelbary AA. Use of novosomes as a vesicular carrier for improving the topical delivery of terconazole: in vitro characterization, in vivo assessment and exploratory clinical experimentation. *IJN*. 2021;16:119–132. doi:10.2147/IJN.S287383
27. Araújo J, Gonzalez-Mira E, Egea MA, Garcia ML, Souto EB. Optimization and physicochemical characterization of a triamcinolone acetate-loaded NLC for ocular antiangiogenic applications. *Int J Pharm*. 2010;393(1–2):168–176. doi:10.1016/j.ijpharm.2010.03.034
28. Schier L, Lima D, Dennison M, Araujo M, Pécio S. Adsorption modeling of Cr, Cd and Cu on activated carbon of different origins by using fractional factorial design Adsorption modeling of Cr, Cd and Cu on activated carbon of different origins by using fractional factorial design. *Chem Eng J*. 2011;166(3):881–889. doi:10.1016/j.cej.2010.11.062
29. Chauhan B, Gupta R. Application of statistical experimental design for optimization of alkaline protease production from *Bacillus* sp. RGR-14. *Process Biochem*. 2004;39(12):2115–2122. doi:10.1016/j.procbio.2003.11.002

30. Kaushik R, Saran S, Isar J, Saxena RK. Statistical optimization of medium components and growth conditions by response surface methodology to enhance lipase production by *Aspergillus carneus*. *J Mol Catal B Enzym*. 2006;40(3–4):121–126. doi:10.1016/j.molcatb.2006.02.019
31. Bendas ER, Abdelbary AA. Instantaneous enteric nano-encapsulation of omeprazole: pharmaceutical and pharmacological evaluation. *Int J Pharm*. 2014;468(1–2):97–104. doi:10.1016/j.ijpharm.2014.04.030
32. El Menshawe SF, Nafady MM, Aboud HM, Kharshoum RM, Elkelay MM, Hamad DS. Transdermal delivery of fluvastatin sodium via tailored spanlastic nanovesicles: mitigated freund's adjuvant-induced rheumatoid arthritis in rats through suppressing p38 MAPK signaling pathway. *Drug Deliv*. 2019;26(1):1140–1154. doi:10.1080/10717544.2019.1686087
33. Guinedi AS, Mortada ND, Mansour S, Hathout RM. Preparation and evaluation of reverse-phase evaporation and multilamellar niosomes as ophthalmic carriers of acetazolamide. *Int J Pharm*. 2005;306(1–2):71–82. doi:10.1016/j.ijpharm.2005.09.023
34. Moawad FA, Ali AA, Salem HF. Nanotransfersomes-loaded thermo-sensitive in situ gel as a rectal delivery system of tizanidine HCl: preparation, in vitro and in vivo performance. *Drug Deliv*. 2017;24(1):252–260. doi:10.1080/10717544.2016.1245369
35. Janoria KG, Gunda S, Boddu SHS, Mitra AK. Novel approaches to retinal drug delivery. *Expert Opin Drug Deliv*. 2007;4(4):371–388. doi:10.1517/17425247.4.4.371
36. Elsherif NI, Shamma RN, Abdelbary G. Terbinafine hydrochloride trans-ungual delivery via nanovesicular systems: in vitro characterization and ex vivo evaluation. *AAPS PharmSciTech*. 2017;18(2):551–562. doi:10.1208/s12249-016-0528-9
37. Sukmawati A, Utami W, Yuliani R, Da'i M, Nafarin A. Effect of tween 80 on nanoparticle preparation of modified chitosan for targeted delivery of combination doxorubicin and curcumin analogue. *IOP Conf Ser Mater Sci Eng*. 2018;311:012024. doi:10.1088/1757-899X/311/1/012024
38. Wang C, Cui B, Guo L, et al. Fabrication and evaluation of lambda-cyhalothrin nanosuspension by one-step melt emulsification technique. *Nanomaterials*. 2019;9(2):145. doi:10.3390/nano9020145
39. Sugawara E, Nikaido H. Properties of AdeABC and AdeIJK efflux systems of *Acinetobacter baumannii* compared with those of the AcrAB-TolC system of *Escherichia coli*. intergovernmental panel on climate change, ed. *Antimicrob Agents Chemother*. 2014;58(12):7250–7257. doi:10.1128/AAC.03728-14
40. Soriano-Ruiz JL, Calpena-Capmany AC, Cañadas-Enrich C, et al. Biopharmaceutical profile of a clotrimazole nanoemulsion: evaluation on skin and mucosae as anticandidal agent. *Int J Pharm*. 2019;554:105–115. doi:10.1016/j.ijpharm.2018.11.002
41. Abdelbary AA, AbouGhaly MHH. Design and optimization of topical methotrexate loaded niosomes for enhanced management of psoriasis: application of Box–Behnken design, in-vitro evaluation and in-vivo skin deposition study. *Int J Pharm*. 2015;485(1–2):235–243. doi:10.1016/j.ijpharm.2015.03.020
42. Varshosaz J, Pardakhty A, Hajhashemi VI, Najafabadi AR. Development and physical characterization of sorbitan monoester niosomes for insulin oral delivery. *Drug Deliv*. 2003;10(4):251–262. doi:10.1080/drdd_10_4_251
43. Devaraj GN, Parakh SR, Devraj R, Apte SS, Rao BR, Rambhau D. Release studies on niosomes containing fatty alcohols as bilayer stabilizers instead of cholesterol. *J Colloid Interface Sci*. 2002;251(2):360–365. doi:10.1006/jcis.2002.8399
44. Shazly G. Niosomes as an oral drug delivery system containing tenoxicam. *Bull Pharm Sci Assiut*. 2015;38(1):19–29. doi:10.21608/bfssa.2015.63170
45. Ruckmani K, Jayakar B, Ghosal SK. Nonionic surfactant vesicles (niosomes) of cytarabine hydrochloride for effective treatment of leukemias: encapsulation, storage, and in vitro release. *Drug Dev Ind Pharm*. 2000;26(2):217–222. doi:10.1081/DDC-100100348
46. El-Nabarawi M, Ali A, Aboud H, Hassan A, Godah A. Transbuccal delivery of betahistine dihydrochloride from mucoadhesive tablets with a unidirectional drug flow: in vitro, ex vivo and in vivo evaluation. *DDDT*. 2016;10:4031–4045. doi:10.2147/DDDT.S120613
47. Roehm NW, Rodgers GH, Hatfield SM, Glasebrook AL. An improved colorimetric assay for cell proliferation and viability utilizing the tetrazolium salt XTT. *J Immunol Methods*. 1991;142(2):257–265. doi:10.1016/0022-1759(91)90114-u
48. Bondaryk M, Kurzątkowski W, Staniszevska M. Antifungal agents commonly used in the superficial and mucosal candidiasis treatment: mode of action and resistance development. *Postepy Dermatol Alergol*. 2013;30(5):293–301. doi:10.5114/pdia.2013.38358
49. Jahn B, Martin E, Stueben A. Susceptibility testing of *Candida albicans* and *Aspergillus* species by a simple microtiter menadione-augmented tetrazolium bromide assay. *J Clin Microbiol*. 1995;33(3):661–667.

International Journal of Nanomedicine

Publish your work in this journal

The International Journal of Nanomedicine is an international, peer-reviewed journal focusing on the application of nanotechnology in diagnostics, therapeutics, and drug delivery systems throughout the biomedical field. This journal is indexed on PubMed Central, MedLine, CAS, SciSearch®, Current Contents®/Clinical Medicine,

Submit your manuscript here: <https://www.dovepress.com/international-journal-of-nanomedicine-journal>

Journal Citation Reports/Science Edition, EMBase, Scopus and the Elsevier Bibliographic databases. The manuscript management system is completely online and includes a very quick and fair peer-review system, which is all easy to use. Visit <http://www.dovepress.com/testimonials.php> to read real quotes from published authors.